Resonance contribution to electron-impact excitation of Ne-like ions

Gaber Omar* and Yukap Hahn
Department of Physics, University of Connecticut, Storrs, Connecticut 06268
(Received 8 July 1987)

Detailed calculation of cross sections and rate coefficients for electron-impact excitation of Ne-like ions is presented in which contributions of the resonance intermediate states, $2p^5n_tl_tnl$ with $n_t \leq 4$, are included, leading to the final states $2p^53l_f$, where $l_f = 0,1,2$. The cascade effect greatly complicates the calculation, as compared with the complementary process, the dielectronic recombination. The present study of the Fe^{16+} ion supplements the earlier work by B. W. Smith *et al.* [Astrophys. J. **298**, 898 (1985)], while the Se^{24+} ion was considered in detail for application to soft x-ray lasers. The resonance-excitation effect reduces substantially the existing discrepancy in the case of Se between the simple ionization-balance model and recent plasma experiments.

I. INTRODUCTION

In electron-ion collision, resonance intermediate states often play a dominant role,[1] as evidenced by many recent studies on ionization[2] [excitation autoionization (EA) versus direct ionization (DI)] and capture[3] [dielectronic recombination (DR) versus radiative recombination (RR)]. Several calculations of the resonant-excitation (RE) cross sections were reported recently,[4–8] which again showed that the resonance mode can dominate over direct excitation (DE) in many cases. The present study[9,10] of the RE process for Ne-like ions was motivated (i) by the recent plasma experiment[11,12] in which the prediction of a simple collisional population model was at variance with the data, suggesting a much higher overall excitation rate for the $2p^53p$ state, and (ii) by the fact that RE is the complementary process to DR, and the latter is of major importance in radiation cooling of high-temperature plasma. Their probabilities are related by $1 = P_{\rm DR} + P_{\rm RE}$. In addition, the soft x-ray laser experiment[11] on Se^{24+} indicated an unusually large $2p^53p$ $(J=2)$ substate population, while the direct-excitation mode leads predominantly to the $J=0$ state. The result of Smith *et al.*[8] in the case of Fe^{16+} indicated that the RE mode populated the $J=2$ and the 0 states by statistical ratio 5:1 at $k_BT_e = 200$ eV, while the total DE rate, including cascade, was twice as large as that of RE, and DE populated the $J=2$ and 0 states by roughly the ratio 1:5. A more recent experiment[13] on Fe^{16+}, Ge^{22+}, and Kr^{26+} also showed a much greater overall population of the $2p^53p$ state than that expected from the direct-excitation rates, by as much as a factor of 2 to 4, but the substate ratio ($J=2$ versus $J=0$) was much more in line with the DE prediction. The main purpose of this paper is to understand some of the processes by which the $2p^53p$ state can be excited.

There are many processes which can contribute to the population of $2p^53l_f$ of Se^{24+}. For example, we have, to lowest order,

$$\begin{array}{l} e + \mathrm{Se}^{25+} \rightarrow \\ e_cl_c + 2p^5 \end{array} \left[\begin{array}{c} \longrightarrow \\ \rightarrow (\mathrm{Se}^{24+})^{**} \rightarrow \\ 2p^43l_fnl \end{array} \right] \begin{array}{l} \quad\quad (\mathrm{RR}) \\ \rightarrow \\ (\mathrm{Se}^{24+})^{*} + \gamma \\ 2p^53l_f \;\; (\mathrm{DR}) \end{array} \qquad \begin{array}{r} (1.1\mathrm{a}) \\ \\ (1.1\mathrm{b}) \end{array}$$

$$\begin{array}{l} e + \mathrm{Se}^{24+} \rightarrow \\ e_cl_c + 2p^6 \end{array} \left[\begin{array}{c} \longrightarrow \\ \rightarrow (\mathrm{Se}^{23+})^{**} \rightarrow \\ 2p^5n_tl_tnl \end{array} \right] \begin{array}{l} \quad\quad\quad (\mathrm{DE}) \\ \rightarrow e' + (\mathrm{Se}^{24+})^{*} \\ \quad 2p^53l_f \;\; (\mathrm{RE\ with\ CI}) \end{array} \qquad \begin{array}{r} (1.2\mathrm{a}) \\ \\ (1.2\mathrm{b}) \end{array}$$

$$\begin{array}{l} e + \mathrm{Se}^{23+} \rightarrow \\ e_cl_c + 2p^63s \end{array} \left\{ \begin{array}{c} \longrightarrow \\ \\ \rightarrow e' + (\mathrm{Se}^{23+})^{**} \rightarrow \\ 2p^53snl \\ \rightarrow (\mathrm{Se}^{22+})^{***} \rightarrow \\ 2p^53sn_tl_tnl \end{array} \right\} \begin{array}{l} \\ \\ \rightarrow (\mathrm{Se}^{24+})^{*} + e'' + e' \\ 2p^53l_f \\ \\ \end{array} \begin{array}{l} (\mathrm{DI}) \\ \\ (\mathrm{EA\ with\ CI}) \\ \\ (\mathrm{REDA\ and\ READ}) \\ \end{array} \qquad \begin{array}{r} (1.3\mathrm{a}) \\ \\ (1.3\mathrm{b}) \\ \\ (1.3\mathrm{c}) \\ \end{array}$$

where CI represents configuration interaction, REDA represents resonance excitation followed by double autoionization,[14] and READ is resonance excitation followed by auto-double-ionization.[15]

In previous studies[12,13,16,17] of Se^{24+} and Fe^{16+}, the following processes are included in the determination of ionization balance; RR, DR, and DE with cascades. In this paper we consider explicitly the RE contribution to the $2p^5 3l_f$ excitation as a possible explanation of the discrepancy in population of the $2p^5 3p$ state mentioned above. In Sec. IV we also discuss several additional processes, EA and DR.

II. RESONANT EXCITATION—THEORY

The basic formulation of the theory for RE is identical to that for DR and we simply refer to Ref. 3 for details, except for the fact that here the cascade transitions play a more important role; their effect is to increase the overall cross section, while the cascade effect reduces the DR cross sections and rate coefficients. Thus, for the Se^{24+} target ion, for example,

$$
\begin{array}{l}
e+\mathrm{Se}^{24+}\to \\
e_c l_c + 2p^6
\end{array}
\left\{
\begin{array}{ll}
\longrightarrow e' + \underset{2p^5 3l_f}{(\mathrm{Se}^{24+})^*}\ \ (\mathrm{DE}) & (2.1\mathrm{a}) \\[2ex]
\to e' + \underset{2p^5 nl}{(\mathrm{Se}^{24+})^*} \longrightarrow \underset{2p^5 3l_f}{(\mathrm{Se}^{24+})^*} + \gamma\,(\text{DE with cascade}) & (2.1\mathrm{b}) \\[2ex]
\to \underset{2p^5 3l_t nl}{(\mathrm{Se}^{23+})^{**}} \longrightarrow \underset{2p^5 3l_f}{(\mathrm{Se}^{24+})^*} + e'(\text{RE with CI}) & (2.1\mathrm{c}) \\[2ex]
\to \underset{2p^5 n_t l_t nl}{(\mathrm{Se}^{23+})^{**}} \to \left\{
\begin{array}{l}
\longrightarrow \underset{2p^5 3l_f}{(\mathrm{Se}^{24+})^*} + e'\ \ (\mathrm{RE}) \\
\longrightarrow 2p^5 n'l' \to 2p^5 3l_f + \gamma\ \ (\text{RE with cascade})\ .
\end{array}\right. & (2.1\mathrm{d})
\end{array}
\right.
$$

In the following all the states labeled by $(d,d',d'',\dots)$ are Auger unstable, while $(f,f',f'',\dots)$ are Auger stable. The RE cross section is defined, in the isolated resonance approximation and in lowest order, by

$$\sigma^{\mathrm{RE}} = \frac{4\pi}{(p_c a_0)^2} V_a(i\to d)\tilde{\xi}(d\to f)\pi a_0^2 \tilde{\delta}\ , \tag{2.2}$$

where the radiationless excitation-capture probability is

$$V_a(i\to d) = \frac{g_d}{2g_i} A_a(d\to i)\ , \tag{2.3}$$

by detailed balance, $A_a(d\to i)$ is the autoionization transition probability, and the partial Auger yield modified by radiative cascade is defined by

$$\tilde{\xi}(d\to f) = \sum_{f'} \frac{A_a(d\to f')X(f'\to f)}{\Gamma_a(d)+\Gamma_r(d)} = \sum_{f'} \xi(d\to f')X(f'\to f)\ . \tag{2.4}$$

The purely radiative cascade branching ratio (special case of ω, when $\Gamma=\Gamma_r$ and $\Gamma_a=0$) is given by

$$X(f'\to f) = \frac{A_r(f'\to f)}{\sum_{f''} A_r(f'\to f'')} = \frac{A_r(f'\to f)}{\Gamma_r(f')}\ , \tag{2.5}$$

where $A_r(f'\to f)$ is the radiative transition probability and

$$\Gamma_a(d) = \sum_{i'} A_a(d\to i'),\quad \Gamma_r(d) = \sum_{f'} A_r(d\to f')\ . \tag{2.6}$$

We have also used in σ^{RE}

$$\tilde{\delta}(E_i - E_d) = \frac{\dfrac{\Gamma(d)}{2\pi}}{(E_i-E_d)^2 + [\Gamma(d)/2]^2} \tag{2.7}$$

with

$$\int de_c \tilde{\delta}(E_i - E_d) = 1\ , \tag{2.8}$$

where $E_i = e_c + e_i$. For presentation of the data, it is convenient to define[3] an energy-averaged cross section

$$\bar{\sigma}^{\mathrm{RE}} \equiv \frac{1}{\Delta e_c}\int_{e_c-\Delta e_c/2}^{e_c+\Delta e_c/2} \sigma^{\mathrm{RE}} de_c' = \frac{4\pi}{(p_c a_0)^2} V_a(i\to d)\tilde{\xi}(d\to f)\pi a_0^2 \frac{1}{\Delta e_c}\ , \tag{2.9}$$

where Δe_c is an energy bin chosen such that the experimental beamwidth Δe_B satisfies $\Delta e_B > \Delta e_c > \Gamma(d)$; otherwise, its value is arbitrary. The RE rate coefficient is defined as a thermal average of σ^{RE},

$$\eta^{\mathrm{RE}} = \langle v_c \sigma^{\mathrm{RE}} \rangle = \left[\frac{4\pi\,\mathrm{Ry}}{k_B T_e}\right]^{3/2} V_a(i\to d)\tilde{\xi}(i\to f)e^{-e_c/k_B T_e}\ , \tag{2.10}$$

where a Maxwellian velocity distribution is assumed for the continuum electrons. Note that $\bar{\sigma}^{\mathrm{RE}}$ and η^{RE} are essentially identical, except for the trivial kinematic and thermal factors.

Further correction to σ^{RE} and η^{RE} is derived by including possible radiative cascade prior to the Auger emission, as

$$\tilde{\zeta}(d\to f)\to\left[\tilde{\zeta}(d\to f')+\sum_{d'}\omega(d\to d')\left[\tilde{\zeta}(d'\to f')+\sum_{d''}\omega(d'\to d'')[\tilde{\zeta}(d''\to f')+\cdots]\right]\right]\chi(f'\to f)\ , \tag{2.11}$$

where

$$\omega(d'\to d'')=\frac{A_r(d'\to d'')}{\Gamma(d')} \tag{2.12}$$

is the partial fluorescence yield. Obviously,

$$\sum_{i'}\zeta(d\to i')+\sum_{j'}\omega(d\to j')=1\ , \tag{2.13}$$

where i' and j' are for all the available states to which the state (d) can decay, either by Auger or by radiative emission, irrespective of their stability. Evidently, by definition of the RE process, the cascade decay of the first intermediate state d is such that only one Auger emission is allowed. Of course, there can be one or more radiative emission before or after the Auger emission. Thus the most general cascade formula for the RE process is

$$\sigma^{\mathrm{RE}}=\frac{4\pi}{(p_c a_0)^2}V_a(i\to d)(1+\omega+\omega\omega+\cdots)\zeta \times(1+\omega+\omega\omega+\cdots)\tilde{\delta}(\pi a_0^2)\ , \tag{2.14}$$

where $\chi=$ special case of ω with $\Gamma=\Gamma_r$ and $\Gamma_a=0$, and all the intermediate-state sums are assumed.

Because of the complicated cascade structure, σ^{RE} and η^{RE} are in general much more difficult to evaluate than the corresponding DR rates, α^{DR}. Nevertheless, the essential structure of σ^{RE} is identical to that of DR; the basic constituent ingredients are still A_a and A_r.

The direct-excitation cross section may be estimated approximately using a simple formula[2]

$$\sigma_{if}^{\mathrm{DE}}=\frac{8\pi}{\sqrt{3}}\frac{f_{if}g'}{e_c\Delta E_{if}}(\pi a_0^2)\ , \tag{2.15}$$

where e_c is the incident electron energy in Ry, ΔE_{if} is excitation energy in Ry, f_{if} is oscillator strength (of hydrogen and hydrogenic ions), g' is Gaunt factor congruent 1 for highly charged ions. Incidentally, the collision strength is defined as

$$\Omega_{i\to f}=g_i\left[\frac{e_c}{\mathrm{Ry}}\right]\sigma_{i\to f}\ , \tag{2.16}$$

where the statistical weights $g_i=\hat{L}\hat{S}$ or $\hat{J}$; $\hat{L}\equiv 2L+1$, etc., and $\sigma_{i\to f}$ is the excitation cross section in units of πa_0^2.

The quantities A_a and A_r are evaluated in this paper using the identical procedure we employed for our DR study;[3,18] the bound orbitals are generated by a nonrelativistic Hartree-Fock (HF) program,[19] in single configuration, while the continuum orbitals are evaluated in the HF distorted potential with nonlocal exchanges. The matrix elements for A_a and A_r are evaluated then in L-S coupling.

For ready comparison, we define an energy-integrated total cross section as

$$S=\sum_d\int^{e_c(\mathrm{th})}\sigma(i\to d)de_c'/\Delta e_c =\sum_d\bar{\sigma}\,[i\to d;<e_c(\mathrm{th})]\ . \tag{2.17}$$

III. RESULTS AND DISCUSSION

The RE cross sections are calculated for Mg^{2+}, Ti^{12+}, Fe^{16+}, and Se^{24+} of the Ne-like ions using the bin $\Delta e_c=0.1$ Ry. The three resonance excitation channels of interest here are the $2p^53l_f$ with $l_f=0,1,2$. We investigated only the $2p^53s$ channel in the case of Mg^{2+} and Ti^{12+} but made a more complete investigation for Fe^{16+} and Se^{24+} by including the $2p^53s$, $2p^53p$, and $2p^53d$ resonance-excitation channels. In all cases, contributions from the intermediate states of the form $2p^5n_tl_tnl$ with $n_t\le 4$ are included in order to reduce the calculation to a manageable level. Our results for the four ions are summarized below.

A. Ti^{12+}

The $2p^53s$ RE cross sections are calculated. The result shows three peaks. The first one is at continuum energies which lie between 460 and 461.5 eV and correspond to the doubly excited intermediate states $2p^53p9p$ and $2p^53d6p$. It has the value 1.27×10^{-18} cm^2 for $\Delta e_c=0.1$ Ry. The second peak comes from the intermediate states $2p^53d6d$ and $2p^53d6f$, and occurs at $e_c=464.5$ eV with the magnitude 3.89×10^{-18} cm^2. We summarize the $2p^53s$ RE cross sections in Table I together with that of the other ions for the same groups of intermediate states, and show the behavior of σ^{RE} with

TABLE I. The integrated $2p^53s$ RE cross sections S for Mg^{2+}, Ti^{12+}, Fe^{16+}, and Se^{24+} at $\Delta e_c=0.1$ Ry. Contributions from dominant groups of autoionizing states lie energetically below the $2p^53p$ threshold. The values for Ti^{12+} (*) were obtained in the AMA approximation.

d Target	$3pns$	$3pnp$ (10^{-19} cm^2)	$3pnd$	n
Mg^{2+}	38.4	43.9	71.2	≥ 4
Ti^{12+}*	3.87	14.4	26.5	≥ 10
Fe^{16+}	1.71	6.38	7.65	≥ 11
Se^{24+}	0.67	1.62	2.47	≥ 13

Z_c (nuclear charge) for the neon isoelectric sequence. The overall $2p^53s$ RE cross section agrees well with the previous calculation of Pindzola *et al.*[6] *The resonance-excitation rate coefficient for the* $2p^53s$ channel at $T_e=14.51$ Ry is $\eta^{RE}(2p^53s)=2.08\times10^{-11}$ cm^3/sec, which is to be compared with 2.14×10^{-11} cm^3/sec, given in Ref. 6.

B. Mg^{2+}

We investigated all the intermediate states which lie between the $2p^53s$ and $2p^53p$ threshold energies. The intermediate states of the form $2p^53pnl$ with $n\geq4$ and $l=0,1,2,3$ contribute to the $2p^53s$ RE channel only, while all the states of the form $2p^53dnl$ are found to lie above the $2p^53p$ threshold and are not included in our calculation. The $2p^53s$ RE cross sections and rate coefficients are calculated for these $2p^53pnl$ autoionizing states with an energy bin of 0.1 Ry, and temperature $T_e=1.75$ Ry. In Table II we present σ^{RE} and η^{RE} for the $2p^53s$ RE.

For the dominant intermediate states $2p^53p4d$ $\Gamma_a(d\to f_1)\approx1.5\times10^{15}$ sec^{-1}, which is 10^3 times larger than $\Gamma_a(d\to i)$, where $i\equiv2p^6$ and $f_1\equiv2p^53s$. That is, $\Gamma_a(d\to f_1)\geq10^5\Gamma_r$. Therefore, $\zeta(d)\approx1$, which makes σ^{RE} large and σ^{DR} small. The ratio of RE and DR cross sections or rate coefficients for this state is

$$\sigma^{RE}/\sigma^{DR}=\eta^{RE}/\alpha^{DR}=\zeta(d)/\omega(d)$$
$$=0.997/0.7\times10^{-5}=1.37\times10^5 .$$

TABLE II. The $2p^53s$ RE cross sections σ^{RE} for $\Delta e_c=0.1$ Ry and rate coefficients η^{RE} at $T_e=1.75$ Ry for Mg^{2+} in LS coupling. All the intermediate states lie below the $2p^53p$ threshold.

e_c (Ry)	d	σ^{RE} (10^{-18} cm^2)	η^{RE} (10^{-11} cm^3/sec)
4.01	$3p5s$	1.43	0.619
4.11	$3p6s$	0.682	0.286
4.17	$3p7s$	0.429	0.180
4.21	$\geq3p8s$	1.30	0.546
3.86	$3p4p$	1.08	0.493
4.05	$3p5p$	1.02	0.429
4.14	$3p6p$	0.638	0.264
4.18	$3p7p$	0.410	0.168
4.21	$\geq3p8p$	1.25	0.519
4.00	$3p4d$	3.00	1.30
4.11	$3p5d$	1.47	0.594
4.17	$3p6d$	0.760	0.308
4.20	$3p7d$	0.467	0.186
4.22	$\geq3p8d$	1.42	0.575
4.02	$3p4f$	0.067	0.029
4.12	$3p5f$	0.054	0.023
4.17	$3p6f$	0.037	0.015
4.20	$3p7f$	0.023	0.038
4.22	$\geq3p8f$	0.069	0.115

As a result, when the $2p^53s$ RE channel is open, both σ^{DR} and α^{DR} are very small. We will return to this point in the case of Fe^{16+} in Table IV.

Since all the $2p^53pnl$ states can decay to $2p^53s$ and all $2p^53dnl$ can go to both $2p^53s$ and $2p^53p$ RE channels by Auger emission, their contribution to σ^{DR} is very small. Hence, the dominant contributions to DR will come mainly from the $2p^53snl$ intermediate states, which are always small. Therefore, the DR cross section corresponding to the L-shell excitation of Mg^{2+} will presumably be on the order of 10^{-23} cm^2. Note that the contribution from $d=2p^53png$ to the $f_1=2p^53s$ RE can be neglected because $\Gamma(d\to f_1)$ is very small ($\approx4\times10^7$ sec^{-1}). For example, we have $\sigma^{RE}=8.4\times10^{-22}$ cm^2 for $d=2p^53p5g$.

C. Fe^{16+}

The contributions to the $2p^53s$, $2p^53p$, and $2p^53d$ RE cross sections and rate coefficients are calculated for the intermediate states $2p^53pn_1l$ with $n_1\geq10$, $2p^53dn_2l$ with $n_2\geq7$, and $2p^5n_1l_1n_2l_2$ with $n_1\leq4$ and $l_1,l_2\leq3$. We summarize the RE cross sections for Fe^{16+} in Fig. 1, and the RE coefficients at $T_e=15.9$ Ry are compared in Table III with the previous work of Smith *et al.*[8] A good agreement was obtained for most of the intermediate-state groups. Some disagreements were found, which were traced to two causes: (i) A slight difference in the orbital energies we used from the configuration mixed values made some intermediate states accessible to RE in our calculations while these states were energetically forbidden in Ref. 8. (ii) They[8] included only the dominant A_r in Γ_r while we have the total Γ_r; this can affect the final result by as much as 50% in some cases, making our η^{RE} smaller.

Since the contributions from the autoionizing states $2p^54l4l'$ were already calculated for the RE, we evaluated the DR rate coefficients for these states at the temperature $T_e=15.9$ Ry. We obtained $\alpha^{DR}=5.24\times10^{-13}$

TABLE III. Comparison of the present calculation of the RE rate coefficients at $T_e=15.9$ Ry with that of Smith *et al.* (Ref. 18) for Fe^{16+}. The core $1s^22s^22p^5$ is assumed in all the d states, for simplicity. All values are cascade corrected.

d	Present work (10^{-13} cm^3/sec)	Smith *et al.*
	$2p^53s$	
$3pns$	1.18	0.98
$3pnp$	6.17	9.62
$3pnd$	10.50	14.4
$3pnf$	2.85	3.65
$3dns$	0.15	0.15
$3dnp$	2.46	2.04
$3dnd$	30.2	28.8
$3dnf$	3.18	3.29
	$2p^53p$	
$3dns$	0.18	0.17
$3dnp$	4.03	3.40
$3dnd$	6.14	7.95
$3dnf$	4.30	5.51

cm^3/sec, which agreed to within 5% with the results of Chen.[20] We especially note that in the theoretical treatment of the RE process, we cannot simply extrapolate to high Rydberg states (HRS) for the estimation of their contribution. A detailed calculation is necessary of energies of all the intermediate states which lie below the $2p^53d$ threshold energy. As shown in Table IV, when resonance states are above the $2p^53p$ RE threshold, for example, both the $2p^53s$ RE and the DR cross sections are reduced because of the decrease in their branching ratios. The group of intermediate states $3dnp$ with $7 \le n \le 9$ contribute to the $2p^53s$ with fairly large branching ratios, $\zeta_1 = 0.52$ and $\omega = 0.39$ for $n = 7$, for example. But the $2p^53p$ RE channel opens at $n = 10$ and ζ_1 decreases to 0.05 and ω to 0.07, because of a large $\zeta_2 = 0.87$. This means that extrapolation to $n > 10$ will overestimate the HRS contribution in the DR total rate by as much as 50%. This effect was found to be about 10% in the case of Mo^{32+} in Ref. 21.

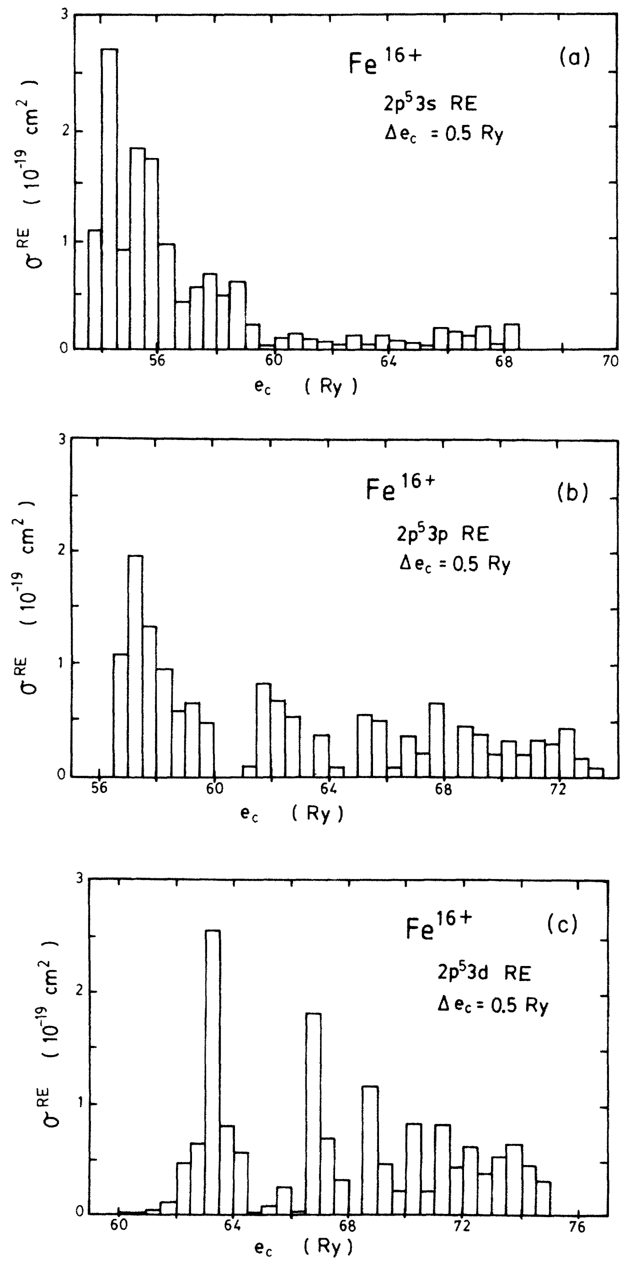

FIG. 1. RE cross sections for Fe^{16+} vs the continuum electron energies e_c (Ry). All values are relative to the $1s^22s^22p^6$ initial ground state of the Fe^{16+} ion. No cascade enhancements are included. (a), (b), and (c) are for the $2p^53s$, $2p^53p$, and $2p^53d$ RE cross sections, respectively.

TABLE IV. RE and DR branching ratios for some intermediate states (d) of Fe^{15+} which decay by Auger emission to the final states $f_1 = 2p^53s$ and $f_2 = 2p^53p$ and by radiative transition to all allowed final states f. The core $1s^22s^22p^5$ is assumed for simplicity. Blank entries imply that Auger emission is not allowed for that n.

d	$\zeta_1(d \to f_1)$	$\omega(d \to f)$	$\zeta_2(d \to f_2)$
$3pns$; $n \ge 11$	0.99	0.003	
$3pnp$; $n \ge 10$	0.98	0.001	
$3pnd$; $n \ge 10$	0.96	0.009	
$3pnf$; $n \ge 10$	0.99	0.004	
$3dns$; $n = 7$	0.82	0.17	
$3dns$: $n \ge 10$	0.08	0.06	0.86
$3dnp$: $n = 7$	0.52	0.39	
$3dnp$; $n \ge 10$	0.05	0.07	0.87
$3dnd$: $n = 7$	0.68	0.23	
$3dnd$; $n \ge 10$	0.16	0.12	0.72
$3dnf$: $n = 7$	0.53	0.39	
$3dnf$; $n \ge 10$	0.07	0.09	0.83

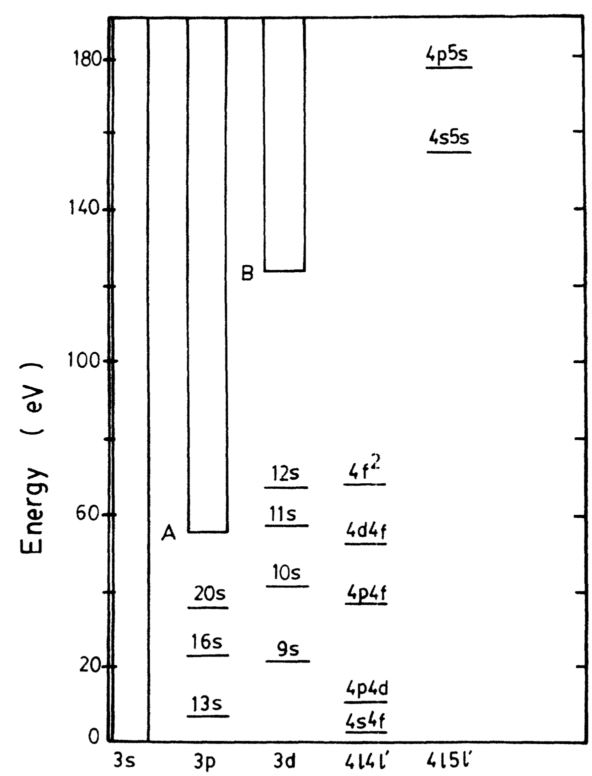

FIG. 2. Energy-level diagram for Se^{23+}. All energies are relative to the $2p^53s$ threshold of Se^{24+}.

TABLE V. Resonance-excitation cross sections σ^{RE} in units of 10^{-20} cm^2 for Se^{24+} with energy bin $\Delta e_c = 0.1$ Ry. The core $1s^2 2s^2 2p^5$ is assumed in d, for simplicity. f_1, f_2, and f_3 are for the $2p^5 3p$, $2p^5 3p$, and $2p^5 3d$ RE channels.

e_c (Ry)	d	f_1	f_2	f_3
107.3	$3p13s$	0.966		
107.8	$3p14s$	0.766		
108.2	$\geq 3p15s$	5.0		
107.3	$3p13p$	2.67		
107.8	$3p14p$	2.12		
108.2	$\geq 3p15p$	13.8		
107.4	$3p13d$	6.4		
107.8	$3p14d$	5.1		
108.2	$\geq 3p15d$	33.0		
107.4	$3p13f$	2.01		
107.9	$3p14f$	2.54		
108.3	$\geq 3p15f$	10.5		
108.3	$3d9s$	0.214		
109.8	$3d10s$	0.117		
110.9	$3d11s$	0.059	0.095	
111.7	$3d12s$	0.046	0.073	
112.3	$\geq 3d13s$	0.256	0.403	
108.5	$3d9p$	2.29		
109.9	$3d10p$	1.27		
110.9	$3d11p$	0.224	4.01	
111.7	$3d12p$	0.173	3.09	
112.4	$\geq 3d13p$	0.952	17.0	
108.6	$3d9d$	17.3		
110.0	$3d10d$	10.2		
111.0	$3d11d$	5.5	5.38	
111.8	$3d12d$	4.3	4.14	
112.4	$\geq 3d13d$	23.5	22.9	
108.7	$3d9f$	3.49		
110.1	$3d10f$	1.94		
111.1	$3d11f$	0.773	7.47	
111.8	$3d12f$	0.595	5.75	
112.4	$\geq 3d13f$	3.28	31.8	
107.0	$4s4f$	2.38		
107.5	$4p4d$	17.8		
109.4	$4p4f$	0.849		
109.6	$4d^2$	9.37		
110.6	$4d4f$	26.7		
111.7	$4f^2$	1.43	6.38	
118.1	$4s5s$	0.19	0.063	0.01
126.4	$4s6s$	0.11	0.036	0.006
131.3	$\geq 4s7s$	0.28	0.091	0.015
119.0	$4s5p$	1.86	0.986	0.157
126.4	$4s6p$	1.08	0.571	0.091
131.3	$\geq 4s7p$	2.74	1.45	0.231
120.0	$4s5d$	0.259	0.022	0.119
127.4	$4s6d$	0.150	0.013	0.069
131.9	$\geq 4s7d$	0.381	0.033	0.175
119.8	$4p5s$	1.05	2.29	0.33
128.1	$4p6s$	0.61	1.32	0.19
133.0	$\geq 4p7s$	1.54	3.36	0.49
120.1	$4p5p$	0.87	23.8	2.19
128.6	$4p6p$	0.41	12.0	0.99
133.3	$\geq 4p7p$	1.04	30.5	2.52
121.6	$4p5d$	0.92	19.9	10.5
129.1	$4p6d$	0.31	11.1	4.23
133.6	$\geq 4p7d$	0.78	28.2	10.7
122.2	$4p5f$	0.015	5.01	0.83
129.4	$4p6f$	0.01	2.90	0.48
133.8	$\geq 4p7f$	0.025	7.37	1.22
121.8	$4d5s$	0.143	0.033	0.311
130.0	$4d6s$	0.083	0.019	0.180
134.9	$\geq 4d7s$	0.211	0.048	0.460
122.6	$4d5p$	0.496	10.05	16.1
130.5	$4d6p$	0.287	5.82	9.33
135.2	$\geq 4d7p$	0.729	14.8	23.7
123.5	$4d5d$	0.604	11.7	70.9
131.0	$4d6d$	0.350	6.77	41.0
135.5	$\geq 4d7d$	0.890	17.2	104.0
124.1	$4d5f$	0.62	2.69	23.3
131.3	$4d6f$	0.36	1.71	13.5
135.7	$\geq 4d7f$	0.91	4.35	34.3
122.7	$4f5s$	0.34	0.075	0.46
131.0	$4f6s$	0.19	0.043	0.26
135.8	$\geq 4f7s$	0.49	0.109	0.66
123.4	$4f5p$	0.011	2.45	0.95
131.4	$4f6p$	0.006	1.42	0.55
136.1	$\geq 4f7p$	0.015	3.61	1.40
124.5	$4f5d$	1.16	2.18	13.8
131.9	$4f6d$	0.673	1.26	7.98
136.4	$\geq 4f7d$	1.71	3.20	20.3
125.1	$4f5f$	0.177	0.787	6.77
132.3	$4f6f$	0.102	0.455	3.92
136.6	$\geq 4f7f$	0.26	1.156	9.96
135.9	$5p^2$	0.148	5.05	0.42
137.9	$5d^2$	0.051	1.97	14.9

D. Se^{24+}

As in the Fe^{16+} case, resonance-excitation cross sections and rate coefficients are calculated for the $2p^5 3l_f$ RE channels with $l_f = 0, 1, 2$. For $l_f = 0$ and 1 all the autoionizing states of the following configurations are included: $2p^5 3pnl$ with $n \geq 13$, $2p^5 3dnl$ with $n \geq 9$, $2p^5 4l4l'$, and $2p^5 4lnl'$ with $n \geq 5$. The dominant contri-

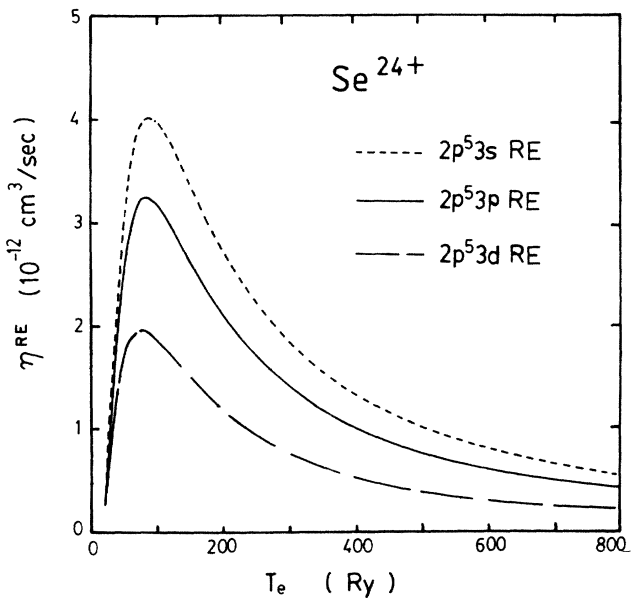

FIG. 3. Total RE rate coefficients η^{RE} for Se^{24+}, in units of 10^{-12} cm^3/sec, for the $2p^5 3s$, $2p^5 3p$, and $2p^5 3d$ RE channels vs the temperature T_e (Ry). Cascade enhancement is included here.

bution to $2p^5 3s$ comes from $2p^5 3dnd$ with $n \geq 13$, while the contribution to the $2p^5 3p$ population comes mainly from $2p^5 4pnp$, $4pnd$, and $4dnp$ with $n \geq 5$. The contribution to $2p^5 3d$ RE channel comes from the $2p^5 4lnl'$ intermediate states with $n \geq 5$, the dominant states of which have $l=2$ and $l'=2,3$. Figure 2 shows the intermediate states which are energetically allowed to contribute to each RE channel. The RE cross sections are summarized (without the cascade effect) in Table V. In addition, the total rate coefficients at several different temperatures T_e are shown in Fig. 3.

IV. CASCADE CORRECTIONS

The results summarized in Sec. II were obtained in the approximation where ζ was evaluated without the cascade corrections. That is, in Eq. (2.14), all the radiative transitions before or after the single Auger emission were neglected by setting the quantities in the two square brackets equal to unity. The total width in the denominator of ζ still contains the full radiative width, however. Obviously, this lowest approximation gives a lower bound; any additional cascade effect will therefore increase the RE cross section.

We illustrate the cascade effect by considering in detail the specific intermediate state $(d)=2p^5 4d5d$ in Se^{23+}, all in the AMA scheme as denoted by overbars. It is one of the more important states that contribute to the $2p^5 3s$ RE by cascade. $\overline{A}_a$ and $\overline{A}_r$ are given in units of sec^{-1}. We have for $i=2p^6+k_c l_c=1,3,5$,

$$\overline{A}_a(d \to i, l_c=1)=1.53(+11) ,$$

$$\overline{A}_a(d \to i, l_c=3)=1.34(+12) ,$$

$$\overline{A}_a(d \to i, l_c=5)=7.63(+9) ;$$

TABLE VI. DE and RE integrated cross sections S for $2p^6 \to 2p^5 3p$ for $J=0$ and 2 in the cases of Fe^{16+} and Se^{24+}. Note the improved ratio for the total cross sections as compared to DE. Additional cascade contributions to RE are estimated to bring this ratio even closer to 1.

	DE		RE (10^{-20} cm^2)		Total	
	Fe^{16+}	Se^{24+}	Fe^{16+}	Se^{24+}	Fe^{16+}	Se^{24+}
$J=0$	781	374	57	27	858	401
$J=2$	160	77	278	134	438	211
Ratio ($J=0/J=2$)	5.0		4.9		1.9	

for $f_1=2p^5 3s+k_c' l_c'=0,2,4$,

$$\overline{A}_a(d \to f_1, l_c'=0)=1.15(+10) ,$$

$$\overline{A}_a(d \to f_1, l_c'=2)=2.31(+10) ,$$

$$\overline{A}_a(d \to f_1, l_c'=4)=5.34(+11) ;$$

for $f_2=2p^5 3p+k_c' l_c'=1,3,5$,

$$\overline{A}_a(d \to f_2, l_c'=1)=1.13(+10) ,$$

$$\overline{A}_a(d \to f_2, l_c'=3)=5.39(+10) ,$$

$$\overline{A}_a(d \to f_2, l_c'=5)=2.15(+12) ;$$

for $f_3=2p^5 3d+k_c' l_c'=0,2,4,6$,

$$\overline{A}_a(d \to f_3, l_c'=0)=2.69(+9) ,$$

$$\overline{A}_a(d \to f_3, l_c'=2)=8.20(+13) ,$$

$$\overline{A}_a(d \to f_3, l_c'=4)=1.65(+12) ,$$

$$\overline{A}_a(d \to f_3, l_c'=6)=2.75(+11) .$$

The total Auger width $\overline{\Gamma}_a=9.35(+13)$ sec^{-1}. The possible radiative rates are

$$\overline{A}_r(d \to f_5=2p^6 5d)=2.07(+12) ,$$

$$\overline{A}_r(d \to f_6=2p^6 4d)=9.06(+11) ,$$

$$\overline{A}_r(d \to d_1=2p^5 3p5d)=2.40(+12) ,$$

$$\overline{A}_r(d \to d_2=2p^5 3p4d)=1.25(+12) ,$$

$$\overline{A}_r(d \to d_3=2p^5 4p4d)=5.06(+11) ,$$

$$\overline{\omega}'(d \to d_3)=0.005 ,$$

$$\overline{A}_r(d \to d_4=2p^5 4p4f)=4.10(+10) ,$$

$$\overline{\omega}'(d \to d_4)=0.004 .$$

The total radiative width $\overline{\Gamma}_r=7.18(+12)$. Therefore, without the cascade effect, we have in AMA,

$$\sigma_{f_1}^{RE}=5.56(-21)\ \text{cm}^2 ,$$

$$\sigma_{f_2}^{RE}=7.33(-20)\ \text{cm}^2 ,$$

$$\sigma_{f_3}^{RE}=8.13(-19)\ \text{cm}^2 .$$

On the other hand,

$$d_3 \to f_1 = 2p^5 3s + l_c', \quad \bar{\zeta}'(d_3) = 0.359 ,$$

$$d_4 \to f_1 = 2p^5 3s + l_c', \quad \bar{\zeta}'(d_4) = 0.542 ,$$

$$\Delta\sigma^{\mathrm{RE}}_{2p^5 3s} \sim (\omega'\zeta' + \omega'\zeta') = 1.95(-21)\ \mathrm{cm}^2 .$$

Therefore, the cascade effect increases the RE cross sections for f_1 by about 35%. In most cases, however, the effect is less drastic. We also note that the $\omega\zeta\omega$-type RE are now possible for the final state $f_1 = 2p^5 3s$, where f_2 and f_3 decay to f_1. The total σ^{RE} for f_1 therefore requires a sum,

$$\sigma^{\mathrm{re}}_{\mathrm{tot}}(f_1) = \sigma^{\mathrm{RE}}(f_1) + \sigma^{\mathrm{RE}}(f_2) X(f_2 \to f_1) + \sigma^{\mathrm{RE}}(f_3) X(f_3 \to f_2) X(f_2 \to f_1) ,$$

where $X(f_2 \to f_1) \sim 1$ while $X(f_3 \to f_2) \sim 0.008$.

V. LSJ COUPLING

Our calculation on Fe^{16+} in LS coupling were summarized in Secs. III and IV, and was in good agreement with that of Smith *et al.*[8] LSJ coupling is required to estimate the specific excitations to $J = 0$ and 2 levels of the configuration $2p^5 3p$ of Se^{24+}, which are of interest to x-ray laser population inversion. We estimated their cross sections by simply taking the appropriate statistical ratio (1:5). The results are summarized in Table VI. We note in particular that for the direct excitation $2p^6 \to 2p^5 3p$ the population ratio of $J = 0$ compared to $J = 2$ states is 4.9 to 1. On the other hand, the sum of the $J = 0$ and 2 population is nearly 82% of the total direct excitation to all the J states of $2p^5 3p$ while it is only 45% of the total in the case of RE. Furthermore, the total direct-excitation cross section is almost 50% larger than that of RE.

Table VI shows that the RE contribution significantly enhances the $J = 2$ population in Se, by as much as a factor of 2. We estimate that additional contribution of approximately 50% of RE calculated here should come from the cascade of higher states which were neglected in our calculation. This makes the relative total population of $J = 0$ and 2 nearly the same. We conclude that significant enhancement in the $J = 2$ populations of the $2p^5 3p$ states of Se^{24+} is achieved by the RE.

VI. CONCLUSIONS

The resonance-excitation cross section and rate coefficients decrease with increasing atomic number in a given isoelectronic sequence. In the RE calculations many threshold energies are close to each other, and this situation requires careful estimation of resonance energies, Auger rates, and HRS contribution. Radiative-cascade effects generally enhance the RE cross sections but decrease the DR process. Improved calculation should include configuration mixing, L-S-J coupling, and other possible relativistic effects. Contributions from the intermediate states which lie above $2p^4 n_1 l_1 n_2 l_2$ levels, with $n_1, n_2 \geq 5$, are also neglected but can be sizable. These are omitted in the present calculation to reduce the work to a manageable level. In the case of Se^{24+} the RE contribution was found to substantially reduce the existing discrepancy in the relative population of the $J = 0$ and 2 states of the $2p^5 3p$. This, together with the contribution from DR (Ref. 12) and EA (Ref. 22), may explain the qualitative feature of the data.[11,12]

ACKNOWLEDGMENTS

One of the authors (Y.H) would like to thank many experimental and theoretical colleagues for numerous discussions on this problem and for sending their results prior to publication, in particular B. W. Smith, B. Whitten, A. Hazi, E. Marmar, J. Terry, and R. Elton. This work was supported in part by a U.S. DOE grant and by the U.S. and Egyptian governments through the AMIDEAST program.

---

*Permanent address: Physics Department, Faculty of Science, Ain Shams University, Cairo, Egypt.

[1]Y. Hahn, Comm. At. Mol. Phys. **13**, 103 (1983).
[2]D. H. Crandall, R. A. Phaneuf, D. C. Gregory, A. M. Howaled, D. W. Mueller, T. J. Morgan, G. H. Dunn, D. C. Griffin, and R. J. W. Henry, Phys. Rev. A **34**, 1757 (1986).
[3]Y. Hahn, Adv. At. Mol. Phys. **21**, 123 (1985).
[4]R. D. Cowan, J. Phys. B **13**, 1471 (1980).
[5]P. Faucher and J. Dubau, Phys. Rev. A **31**, 3672 (1985).
[6]M. S. Pindzola, D. C. Griffin, and C. Bottcher, Phys. Rev. A **32**, 822 (1985).
[7]G. A. Doschek, U. Feldman, and J. F. Seely, J. Appl. Phys. **58**, 3984 (1985).
[8]B. W. Smith, J. C. Raymond, J. B. Mann, and R. D. Cowan, Astrophys. J. **298**, 898 (1985).
[9]Gaber Omar, Y. Hahn, I. Nasser, and Ali H. Moussa (unpublished).
[10]Gaber Omar and Y. Hahn, Bull. Am. Phys. Soc. **32**, 42 (1987).
[11]M. D. Rosen *et al.*, Phys. Rev. **54**, 106 (1985).
[12]D. L. Matthews *et al.*, Phys. Rev. **54**, 110 (1985).
[13]J. Terry and E. Marmar (private communication).
[14]K. LaGattuta and Y. Hahn, Phys. Rev. A **24**, 2273 (1981).
[15]R. Henry, J. Phys. B **12**, L309 (1979).
[16]B. Whitten *et al.*, Phys. Rev. A **33**, 2171 (1986).
[17]J. P. Apruzese *et al.*, Phys. Rev. Lett. **55**, 1877 (1985).
[18]Gaber Omar and Y. Hahn, Phys. Rev. A **35**, 918 (1987).
[19]C. Froese Fischer, *The Hartree-Fock Method for Atoms* (Wiley, New York, 1977).
[20]Y. Hahn, J. Gau, G. Omar, and Dube, Phys. Rev. A **36**, 576 (1987).
[21]M. H. Chen, Phys. Rev. A **34**, 1073 (1986).
[22]W. H. Goldstein, B. L. Whitten, A. U. Hazi, and M. H. Chen (unpublished).